Proceedings World Geothermal Congress 2020+1
Reykjavik, Iceland, April - October 2021

Contributions to the Preliminary Characterization of the Geothermal Potential in the Area of the Galeras Volcano, Colombia.

Julian O. Romero

joromeror@unal.edu.co

Keywords: Geothermal development, geothermal potential, resource assessment, early conceptual model.

ABSTRACT

The present work makes a first approach towards the characterization of the geothermal potential in the Galeras Volcano area starting from the tentative definition of the dynamic qualities and interactions of the basic constituents associated to the existence of its geothermal system. For this purpose, a joint analysis and interpretation of information provided by previous geological, geochemical and geophysical studies is developed with a geothermal criterion defining features such as the extension and location of the heat source, the possible fluid discharge and recharge zones, and their circulation pattern; the lithological units that could constitute a geothermal reservoir and/or a seal layer; the presumed origin of hydrothermal manifestations and their relationship with the heat source. The highlights of this analysis are: 1.The existence of a transitory magmatic chamber, with crust contribution and moderate differentiation and a primary magmatic chamber of basic composition at an estimated depth greater than 13 km 2. The conditioning of the fluid circulation pattern by the Buesaco Fault 3. The NW and SE sectors of the volcanic edifice as the regions of greatest interest for future studies of geothermal prospecting.

1. INTRODUCTION

At present, almost 67% of Colombia's energy demand is supplied by hydroelectric generation, while the remaining 33% is generated by thermoelectric plants. Although Colombia is considered to have great potential and water wealth, the diversification of the national energy matrix is essential to face challenges such as variability and climate change that compromise the energy market, in addition to the prevailing global necessity to promote the development of cleaner energies. Geologically, within the framework of the Pacific ring of fire, Colombia presents a favorable configuration, where the anomalous geothermal gradient is expressed in multiple volcanic manifestations (at least 20 well recognized), and many of them could be appropriate for geothermal development. This potential is observed in Chiles, Cerro Negro, Cumbal, Azufral, Galeras, Doña Juana, Sotará, Puracé, Nevado del Huila, Nevado del Ruíz and Nevado del Tolima volcanoes with the presence of hot springs, hydrothermal alteration zones and fumaroles (ISAGEN, 2014). The Colombian government, in its National Energy Plan 2010 - 2030 and Law 1450 of 2005, sets goals such as expanding and guaranteeing the supply of energy with accessible prices, with quality and reliability standards and incorporating new generation technologies and promoting the use of non-conventional energy sources, among others.

The Galeras Volcanic Complex (GVC) with an evolutionary history of 1.1 ± 0.1 Ma (Calvache, 1990) is part of the so-called inter-Andean depression between the Western and Central mountain ranges (Acosta 1983). The Galeras Volcano (GV) is an active stratovolcano with an estimated age of 4.5 K years, its crater of 320 m radius is the most recent eruptive center of the GVC (Ramírez, 1981) located at coordinates 1° 13' 43.8" N latitude and 77° 21' 33.0" W longitude, 9 km west of the city of Pasto in the department of Nariño, southwestern Colombia. The galeras volcanic edifice reaches a maximum height of 4276 meters above sea level. Its activity is characterized by the occurrence of gas and ash emissions, andesitic lava flows and Vulcanian eruptions that have generated fall deposits and pyroclastic flows; its provents are generally andesitic of the calcoalkaline series, rich in silica (Calvache, 1990)

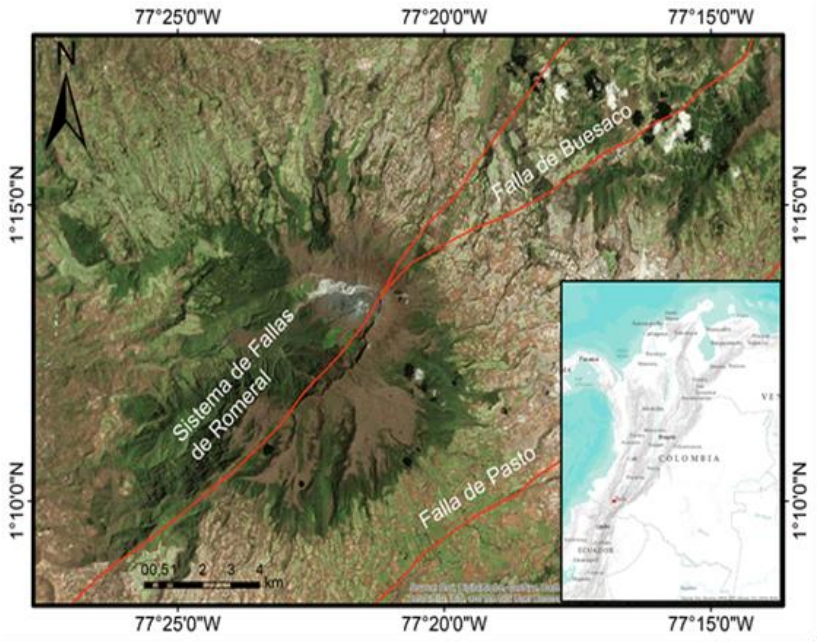

Figure 1: Area of study, Galeras Volcano

2. GEOLOGICAL SETTING

2.1 Structural Features

The regional tectonic configuration is complex, resulting from the collision between the Nazca and South American plates causing the uplift and volcanism of the Andes. Several tectonic features of regional importance converge in the GVC area, including the Romeral Fault System (RFS), which includes four faults, from W to E: Silvia-Pijao Fault (strike of N35º-40ºE) between the GV and the Juanambú River; Buesaco Fault (strike of N40º-65ºE) at NE of the volcano; Pasto Fault (strike of N35º-50ºE) and San Ignacio Fault. The Río Magdalena Fault System (MRFS) has curved fault traces with NE to EW directions that intercept the RFS in the sector of Tangua (12 km south of the GV). The Cauca Fault System (CFS) includes a set of faults striking in the N-NE direction associated with the vertical displacement of greenstone stocks (Murcia and Cepeda, 1984).

Cepeda (1986), recognizes two clearly differentiable groups of calderas. The South Group includes "La Concha, a NE-SW oriented caldera with a diameter of 4.2 km, and La Honda, a NE-SW oriented caldera with a 2.5 km diameter, both with collapse structures in the W direction draining towards the Güaitara River; the North group consists of a main caldera (4.8 km diameter) with two secondary calderas developed on the E border: Genoy with a diameter of 2.2 km and estimated age of 56 K years; and Urcunina caldera (which houses the GV) with a 1.7 km radius and an estimated age of 40 Ka. Calvache (1995). All the north group is elongated in NNE direction, with a scarp of up to 1.6 km and collapse structures in a W direction draining towards the Azufral River.

2.2 Lithology and Chronostratigraphy

The GVC is built on a layer of undifferentiated volcanic and volcanoclastic deposits, which lie on top of Esmitia Formation (Upper Eocene), a sedimentary unit characterized as intercalations of limestones, sandstones, conglomerate sandstones and polymictic conglomerates (León et al., 1979). Descending stratigraphically are meta-sedimentary rocks and Cretaceous diabases with associations of meta-basalts and Paleozoic metamorphic rocks, mostly basic lavas of tholeiitic composition, pyroclastic rocks and sedimentary rocks of marine origin, all intensely folded and faulted. These lithologies are exposed in the Guáitara and Chacagüaico rivers, to the northwest of the GV (Cepeda, 1991). The basement of the area is made up of green schists and quartzites belonging to the Buesaco Paleozoic sequence; these are underlain by high grade metamorphic rocks of Precambrian age called the La Cocha-RíoTellez Migmatitic Complex.

Calvache (1995) carried out a detailed study which delimits six evolutionary phases for the Galeras Volcanic Complex, as well as an event that formed a cone with contrasting characteristics to the entire GVC. To summarize, the evolutionary history of the Galeras Volcanic Complex is more than one million years, and includes two caldera forming events (Genoy and Urcunina), the formation of a slag cone (La Guaca), and at least one collapse of the edifice during the Urcunina stage apparently not related to volcanic activity but to instability due to hydrothermal alteration (López & Williams, 1993).

2. GEOCHEMICAL STUDIES

2.1 Geochemistry of Fumarolic Discharges

Since the reactivation of Galeras Volcano in early 1988 until 1995, Fischer et al. (1996: 1997) performed sporadic geochemical sampling of fumaroles and hot springs. In general, the gas composition of fumaroles is dominated by H_2O, CO_2, SO_2 and H_2S with lower amounts of HCl of magmatic origin. Variations in the concentrations of inert gases N_2, Ar, and He associated with the existence of a basaltic body at depths greater than 6 km were identified, for all these gaseous species a thermodynamic range of equilibrium between 260ºC (hydrothermal system) and 600ºC (intrusive body) was estimated (Fischer et al. 1997). The location of the fumaroles associated with Galeras Volcano and their equilibrium temperature are shown in Figure 2.A. Appendix A summarizes the chemical composition in mmol/mole dry steam of the samples taken by Fischer et al. (1997), with the exception of Pandiaco fumarole, all samples of the study report more than 90% by weight of H_2O, followed in abundance by CO_2, total sulfur ($SO_2 + H_2S$), HCl, N_2, H_2, with lower amounts of HF, He, Ar, CH_4 and O_2. The relative CO_2, ($SO_2 + H_2S$) and HCl contents are shown in Figure 2.B

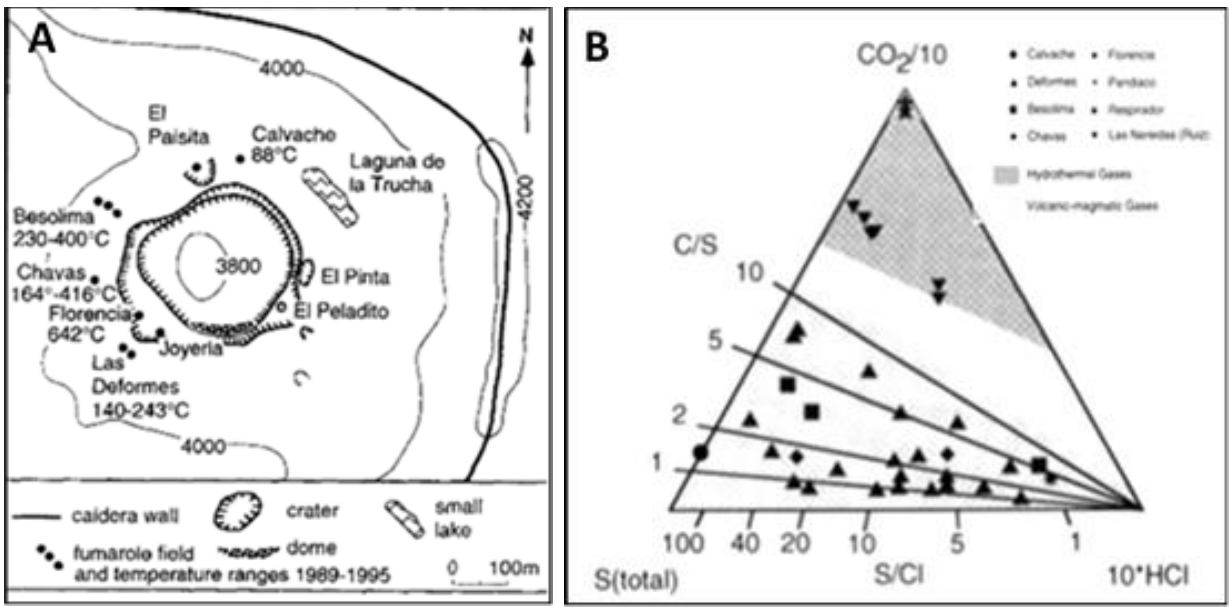

Figure 2 (A) Map of fumaroles in Galeras Volcano area (B) Triangular diagram of abundance of CO_2, S_T and HCl in Galeras Volcano's fumaroles. Taken from Fischer et al. 1997

The of CO_2 - S_T - HCl triangular diagram is useful to distinguish between the gases of volcano-magmatic origin, rich in S and HCl, versus the gases of hydrothermal origin, rich in CO_2 (zone of the graph in which Galeras Volcano`s fumaroles are located), with a C/S radius less than 10, typical of andesitic volcanoes (Symonds & Reed, 1993). The concentrations of H_2O, H_2, CH_4 and CO in the gas samples are used to estimate the subsurface temperatures associated with each fumarole, based on the equilibrium state of the redox reactions in which these species participate. Figure 3.A presents the variation of the H_2/H_2O molar ratio versus measured outlet temperature, while Figure 3.B shows H_2/H_2O and CO/CO_2 molar ratios for evaluation of equilibrium temperatures; Figure 3.C indicates the subsurface equilibrium temperatures calculated for CO/CO_2 and CH_4/CO_2 molar ratios

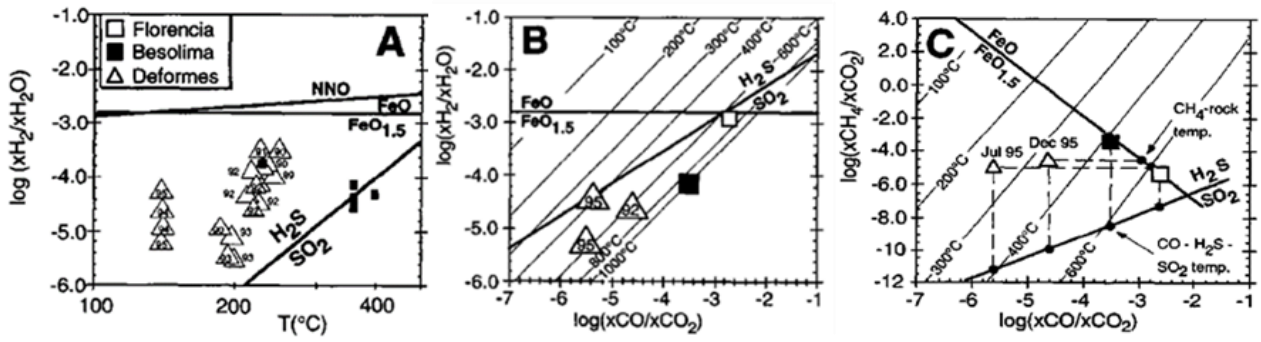

Figure 3 (A) Variation of the H_2/H_2O molar ratio versus measured outlet temperature. (B) H_2/H_2O and CO/CO_2 molar ratios for evaluation of equilibrium temperatures (C) Subsurface equilibrium temperatures calculated with CO/CO_2 and CH_4/CO_2 molar ratios. Taken from Fischer et al., 1997.

The variation in equilibrium temperatures calculated for the Deformes fumarole samples suggests an intense interaction between the magmatic gases, the hydrothermal system and the meteoric water in the subsurface of this part of the volcanic edifice; conversely the Florence and Besolima fumaroles located on the faulted line that crosses the crater report higher and more uniform temperatures. (Fischer et al, 1996). In the case of the Besolima fumarole, the equilibrium temperature calculated for the CO - H_2S - SO_2 ratio is significantly higher than the equilibrium temperature calculated for the CH_4 - rock ratio, indicating that its gases come from shallow levels of the magmatic-hydrothermal system; in contrast to the equilibrium temperatures calculated for the same concentration ratios in the Deformes fumarole, which suggest greater depths of origin for its gases. Fischer et al (1996) recorded that weeks prior to the eruption of July 16, 1992 the H_2O/CO_2 ratio increases, while the HCl/CO_2 and S_T/CO_2 ratios decrease; the authors associated these changes to the selective absorption of S and HCl as a consequence of the sealing of vents in the system.

2.2 Hot Spring's Chemistry

Fig 8 shows the location of springs and water discharges in the vicinity of Galeras Volcano that have been sampled by Fischer et al . (1997). The highest surface spring discharge temperature is reported in the waters of Pandiaco with 31ºC and neutral pH, this feature is located in the limits of the city of Pasto. The Aguas Agrias spring located at 2800 m.a.s.l. on the northeastern flank of the GV, has temperatures between 27 and 29 ºC with pH close to 2 and flow rates less than 1Kg/s. Agua Tibia is the closest spring to the top of the volcanic edifice at 3000 m.a.s.l. located on the west flank, its temperature and pH value are close to 23ºC and 5 respectively, with a flow rate of 30 Kg/s. The Fuente Blanca spring, located in the upper valley of the Azufral River at 2500 m.a.s.l. reports the highest flow rate (300 Kg/s) and pH values of 6. The Guaico Hot Spring in the town of Consaca (1600 m.a.s.l.) to the west of Galeras Volcano has discharge temperatures of 23ºC, neutral pH and flow rates close to 1 Kg/s.

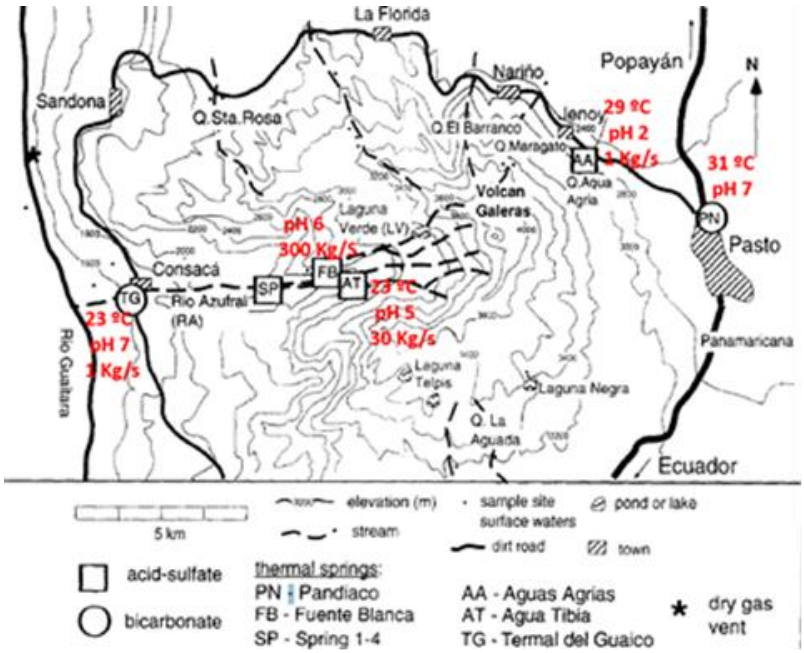

Figure 4 (A) Map of the Galeras Volcano sampled springs, indicating some of the chemical parameters. Modified from Fischer et al. 1997

The classification of these waters according to their relative contents of SO_4, Cl and HCO_3 is presented in Figure 5.A. The discharges from Pandiaco and Guaico are catalogued as bicarbonate waters, while the rest of the samples are acid-sulfate. The SO_4 vs Cl diagram (Fig 5.B) is useful for distinguishing mixing or dilution processes in thermal manifestations, in this case all samples classified as acid-sulfate are relatively aligned, suggesting they are all the result of different degrees of dilution from a common source rich in sulfates and chlorides. The Pandiaco and Guaico hot springs have neutral pH, low Cl and SO_4 contents, but high concentrations of HCO_3, characteristics of waters with high CO_2 dilution. In the case of Aguas Agrias, there is an important variation in its Cl and SO_4 contents, indicating that the Galeras Volcano is an immature hydrothermal system that responds quickly and intensely to changes in the magmatic system (Fischer et al. 1997).

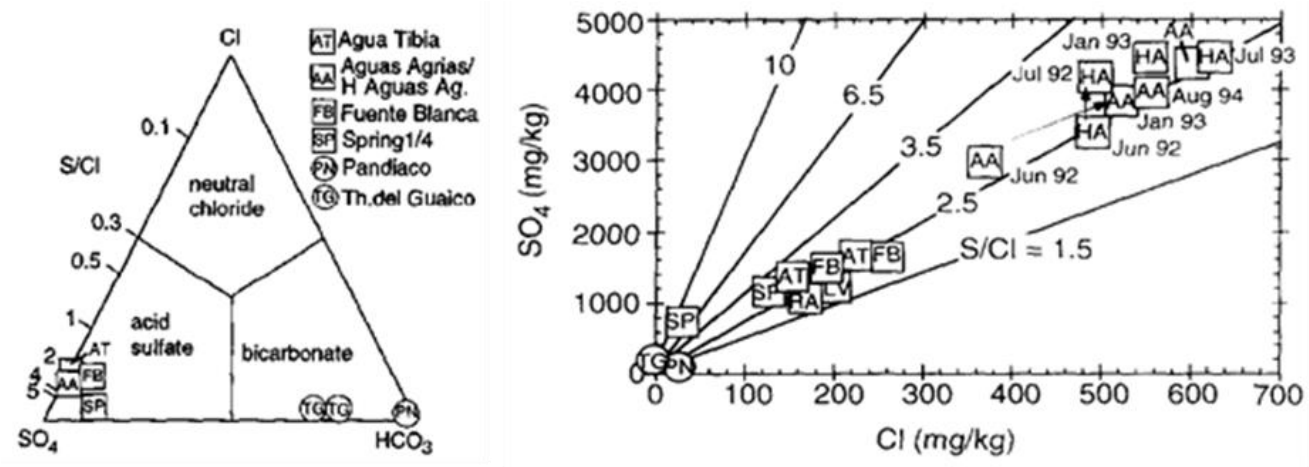

Figure 5 (A) Triangular diagram of SO_4, Cl and HCO_3 for water classification. (B) Cl vs SO_4 concentrations to evaluate water dilution processes. Taken and modified from Fischer et al., 1997

The capture of magmatic volatiles in geothermal and meteoric waters near the volcanic body generates **acid-sulfate** hot springs**,** capable of dissolving the rock and consequently enriching itself in cations; on the other hand, **bicarbonate waters** are present at greater distances from the volcanic center, with lower dissolution capacity and lower concentration of cations and CO_2. The closeness and chemical similarity of the Agua Tibia and Fuente Blanca discharges suggest a common or closely related source; conversely, the difference in the concentration of cations in Aguas Agrias with respect to all other sources suggests the occurrence of an intense chemical dissolution of rock in these waters (Fischer et al. 1997).

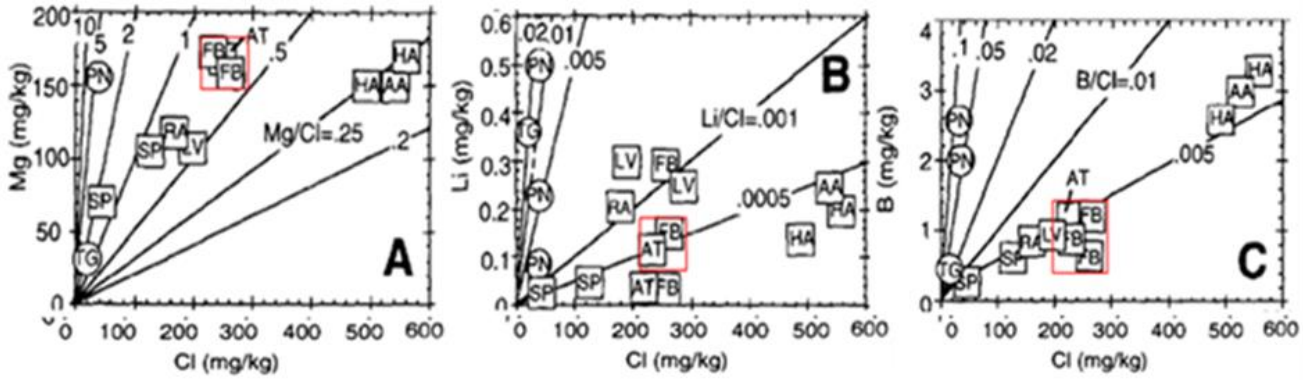

Figure 6 (A) Concentration of some cations versus Cl in hot springs and acid surface waters (Laguna Verde and Rio Azufral) of Galeras Volcano. Taken and modified from Fischer et al., 1997.

The isotopic compositions of the fumaroles and springs of Galeras Volcano are compiled in Appendix B. In summary: samples are located in the mixing zone between the local meteoric line and waters related to a magmatic component responsible for the boiling of aquifers within the volcanic edifice; (Taran & Pokrovsky, 1989) call this component "andesitic water" while (Giggenbach, 1992) calls it "arc type water". The $\delta^{18}O$ vs δD values of the spring samples are presented in Figure 7, the acid-sulfate waters are enriched in ^{18}O due to their greater dissolution capacity during the water-rock interaction.

2.3 Geothermometers

Theoretically, geothermometers represent the fluid-mineral equilibrium in the reactions that depend on temperature. The concentration of some chemical species has been used to define correlations between different elements that allow for the estimation of temperature for a fluid based on the concentration of certain chemical species. According to Yock A. (2009) for the use of geothermometers it is necessary to assume that:

- There is a fluid - mineral equilibrium at depth and its reaction temperature is depth-dependent.
- There is a constant supply of solid phase so that the fluid can be saturated with ions used in geothermal calculations.
- The ascent of the fluid was rapid and there is an insignificant rebalance as it ascends to the surface.
- No mixture with other hot or surface fluids occurs.

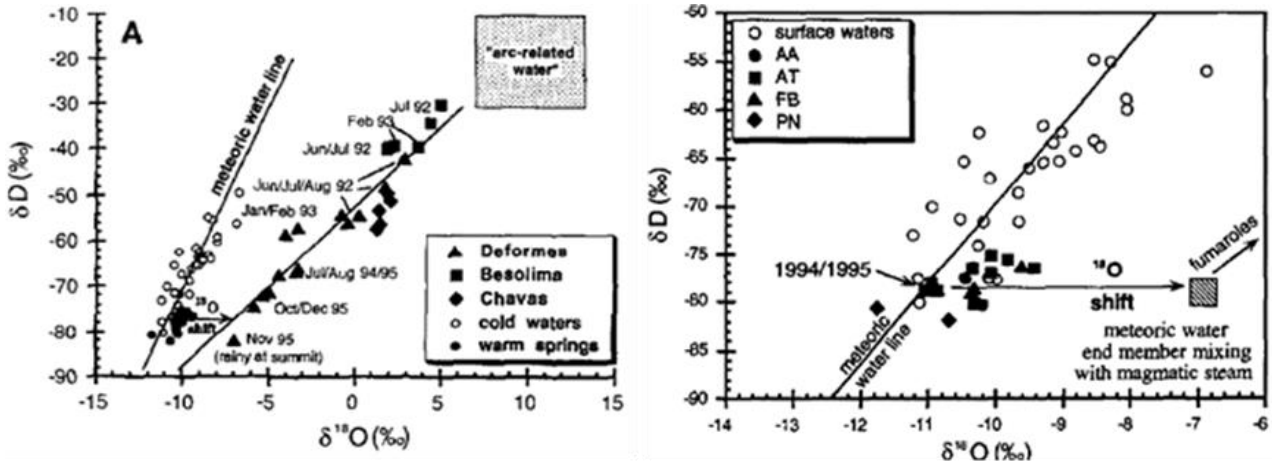

Figure 7 Diagrams δ18O vs δD for samples of Galeras Volcano hot springs and fumaroles. Taken from Fischer et al., 1997

The results of several chemical geothermometers are presented in Table 1. The Na/K geothermometer is most effective in fluids with temperatures above 150°C (Kharaka and Mariner, 1989), explaining why the calculated high temperatures are unreliable. In contrast, the temperatures calculated for the Mg/Li and K_2/Mg geothermometers are lower but reliable. Without considering the Na/K geothermometer, the estimated reservoir temperatures of the hot spring fluids are between 40 and 160 ºC for Agua Tibia and Fuente Blanca, 32 to 48 ºC for Pandiaco and 48 to 200 ºC for Guaico hot spring. It is not convenient to use geothermometers in acid waters (Fournier 1981; Giggenbach 1988) discarding, in the case of Galeras Volcano, the sources of Aguas Agrias. The wide range of temperatures calculated by geothermometers is another evidence of the thermodynamic imbalance of geothermal waters, and the immaturity of the hydrothermal system associated with Galeras Volcano.

DATE	Fuente Bl. 93/01/20	Agua Tibia. 93/03/18	Pandiaco 93/01/17	Pandiaco 93/02/15	Tr Guaico 93/03/19
Discharge temperature	22	27	31	31	23
SiO_2 (a)	88	104	131	132	103
SiO_2 (b)	87	105	135	137	104
~~Na/K (a)~~	223	213	247	250	267
~~Na/K (e)~~	212	198	261	265	283
Mg/Li (d)	37	18	32	47	56
K2/Mg (e)	42	41	54	54	48
Na-K-Ca (f)	154	161	186	187	200
(a) Amorsson et al. (1983). (b) Fournier (1981). (c)Truesdell (1976). (e) Giggenbach (1988). (f) Fournier and Truesdell (1973).					

Table 1 Calculated temperatures with geothermometers. Fischer 1997

3. GEOPHYSICAL SURVEYS

3.1 3D Seismic Tomography

A wide variety of seismic-volcanic signals generated by processes such as cleaning and opening of volcanic conduits, hydrothermal activity, magmatic intrusions, construction and destruction of domes, etc. are recorded. The volcano-tectonic (VT) seismic events associated with extension or shear fracturing in the solid part of the volcano due to pressure induced by magma (Latter, 1979) and (Chouet, 1996); the Tremor episodes (TRE) and Long Period (LP) earthquakes, which are related to fluid dynamics processes in the magmatic and hydrothermal system producing perturbations by transient pressures and resonance of vents or cavities (Chouet, 1981, 1988, 1992 and 1996); a third type corresponds to the so-called Hybrid earthquakes (HIB) which are interpreted as a combination of processes: volumetric changes or transport of fluid material that almost simultaneously induce solid rock fracturing (Chouet, 1992 and 1996).

Carcolé et al (2006) evaluated the spatial distribution of S-wave dispersion for 1564 records of shallow earthquakes (depths less than 10 km) while Vargas et al (2006) analyzed the spatial variation of 2855 coda wave values (Qc) associated with 435 events between September 1989 and June 2002, detected by a network of 19 seismic stations distributed in a range less than 10 km from the Galeras Volcano crater (Figure 12.A). The location of the 435 earthquakes used is shown in Figure 12.B. Seismic events of local magnitude greater than 2.0 were discarded to avoid records affected by saturation. The hypocenters were determined with the software HYPO71 (Lee & Lahr, 1975) and the velocity model by Pasto's Volcanological Observatory.

Vargas et al (2006) define at least three anomalous attenuation zones (Figure 9) that suggest the existence of multiple magmatic bodies; these zones are located to the Southeast, Southwest and Northwest with geometric centers at depths ≥ 13 km for SE and SW and 9 km for the NW case. Multiple minor anomalies reflect a connection between these 3 main zones. It is possible that this connection is controlled in depth by the lineament of the Buesaco and Silvia Pijao faults. An important volume of magma is identified at a depth of ≥ 13 km, tentatively through a system of fractures feeds a smaller magmatic chamber closer to the surface.

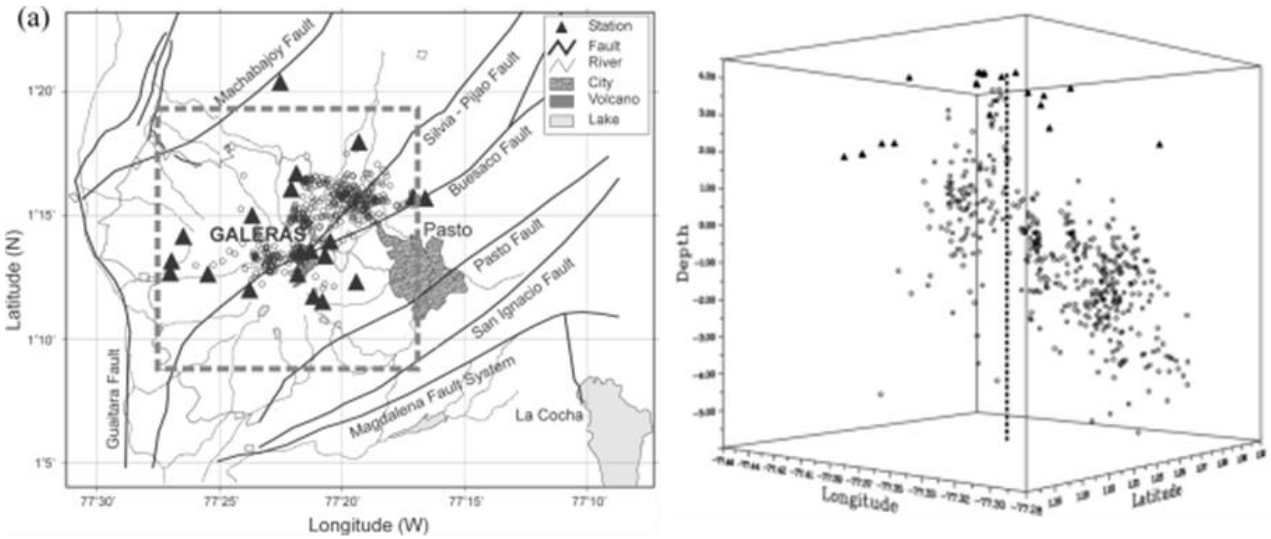

Figure 8 Location of the seismological stations and earthquakes used for 3D tomography and their horizontal projection on the study area surface. Taken from Carcolé et al., 2006

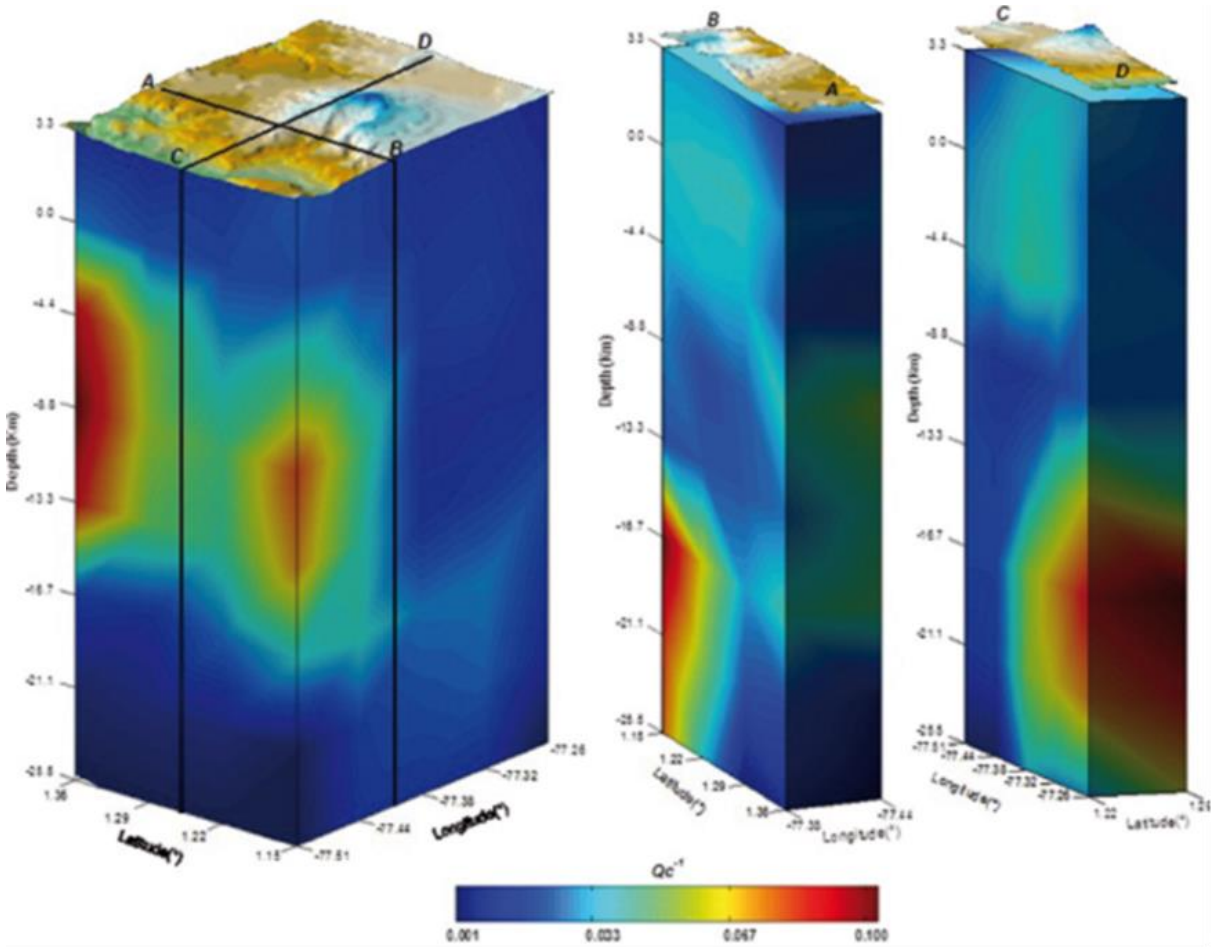

Figure 9 Location of depth coda attenuation distribution for Galeras Volcano Taken from Vargas et al., 2006.

Torres (2012) performed a 3D seismic tomography based on P-wave velocities calculated in the Galeras Volcano area. Figure 10 summarizes the results: high seismic velocities, close to 3.5 km/s, predominate in the active crater. At an elevation of 2 km above sea level there is a low velocity zone towards the NW of the main crater with values between 3 km/s and 2.75 km/s; also, there is a southern low velocity zone with values around 2.9 km/s. At sea level, the low velocity zones of NW and S are slightly more extended; to the NE just below the fault lines of Buesaco and Silvia-Pijao, a high velocity zone (4.3 km/s) is recognized. This zone extends down to the main crater. The W-E and S-N cross sections schematically depict two zones of low velocity, (NE and SW) at depths between 2 and 3 km, in the middle of these zones, even under the main crater, a zone of greater velocity is observed.

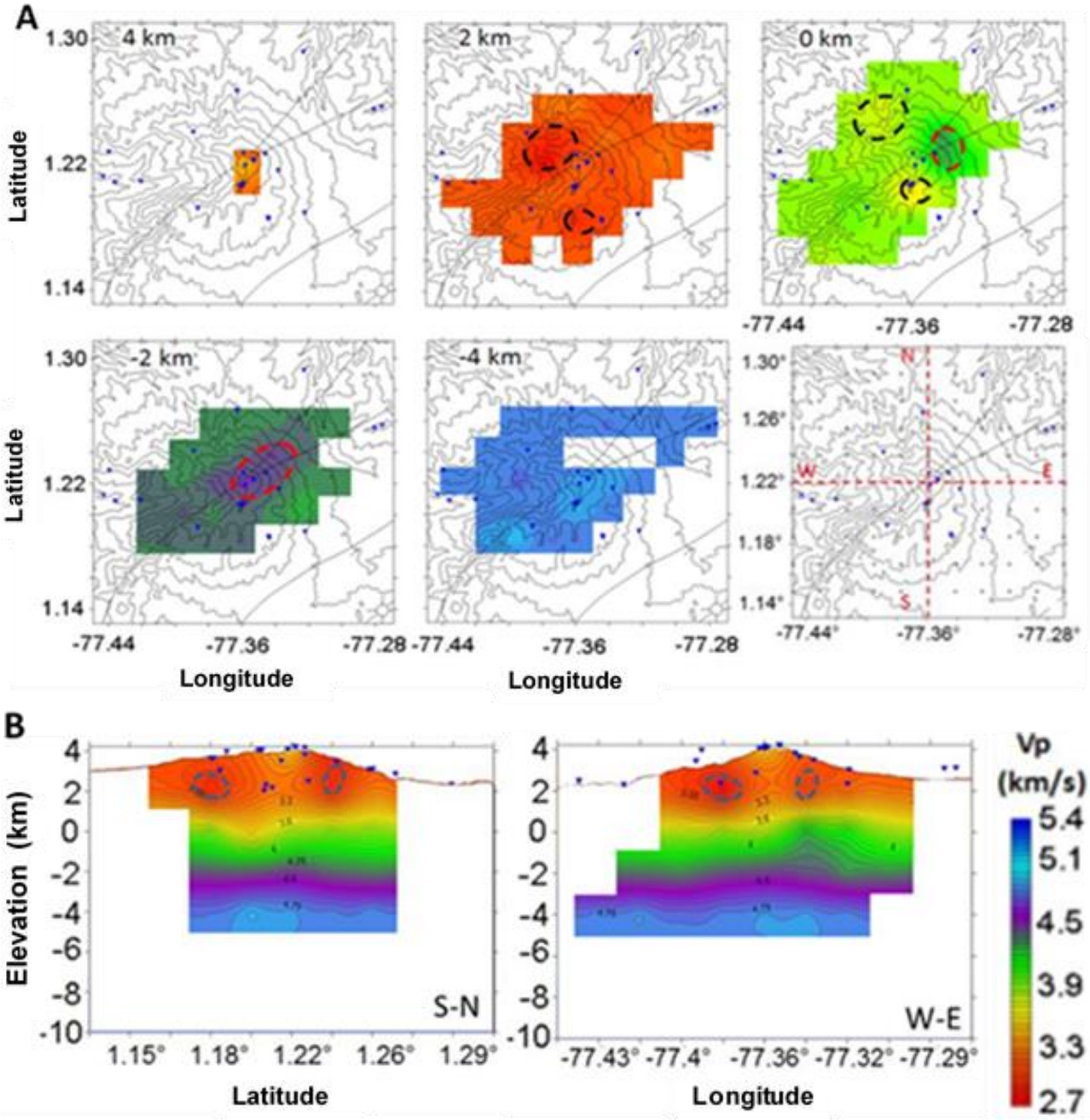

Figure 10 (A) Horizontal sections, P-wave velocity tomography, black and red ellipses enclose low and high velocity zones, respectively. (B) Transversal sections, P-wave velocity tomography. Seismic stations represented by blue triangles. Taken and modified from Torres, 2012.

3.2 Spatial distribution of "B" Parameter

Sánchez et al (2005) analyzed 8435 well-localized seismic events to explore sub-surface structures based on "b" values associated with the frequency-magnitude distribution of seismic records. When graphing the seismic accumulation versus its magnitudes, "b" value represents the slope of the line of best fit for the data. In the earth's crust the b values are close to 1 (Frolich & Davis, 1993) but in volcanic regions this value is frequently higher (Wiemer et al., 1998; Sánchez et al., 2004). This difference has been attributed to a high heterogeneity of materials (Mogi, 1962), areas of less effective stress (Scholz, 1968), areas of high pore pressure (Wyss, 1973) or areas with a high thermal gradient (Warren & Latham, 1970).

The histogram of number of events versus their magnitude shows a simple bell distribution, with some peaks, but uniform tendency (Figure 11.A), with the majority of earthquakes between 1.0 - 1.5 M_L. The diagram of distribution frequency - magnitude (Figure 11.B) shows the slope of adjustment calculated for events with $M_L \geq 1.2$, being b = 1.15.

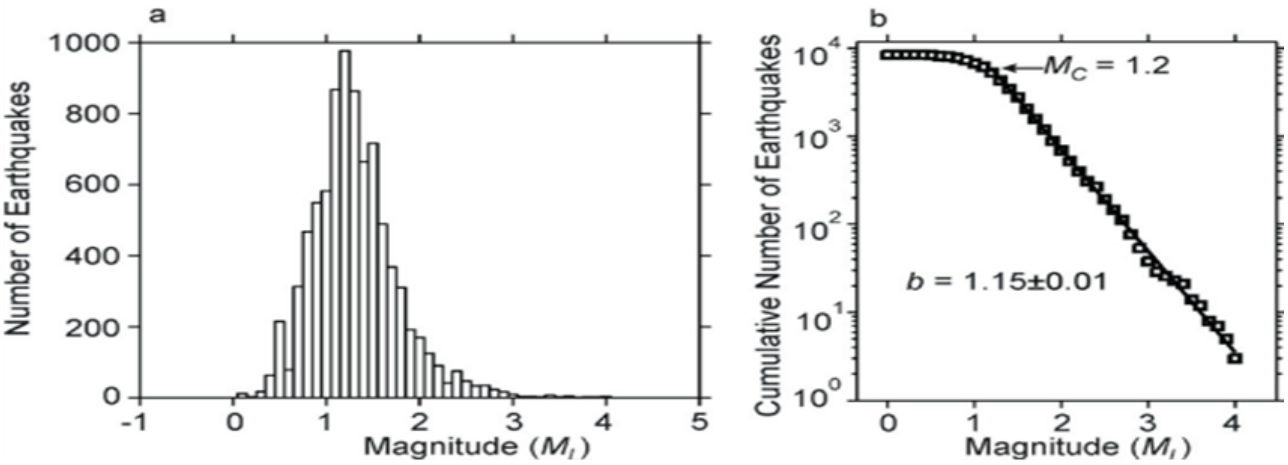

Figure 11 (A) Histogram of number of events versus their magnitude (b) Distribution diagram Frequency - Magnitude. Taken from Sánchez et al., 2005

The three-dimensional distribution of the b-values for Galeras Volcano is shown in Figure 12, denoting a region of high b-values, vertically elongated, distinguishable up to 5 km deep, starting just below the active crater. This anomaly zone may be associated with high pore pressures, constant intrusions and/or eruptions, high material heterogeneity (such as a fracture zone), so it could be a region of volcanic conduits, a transient magma reservoir, or the remnants of a semi-crystallized magmatic intrusion (Sánchez et al 2005).

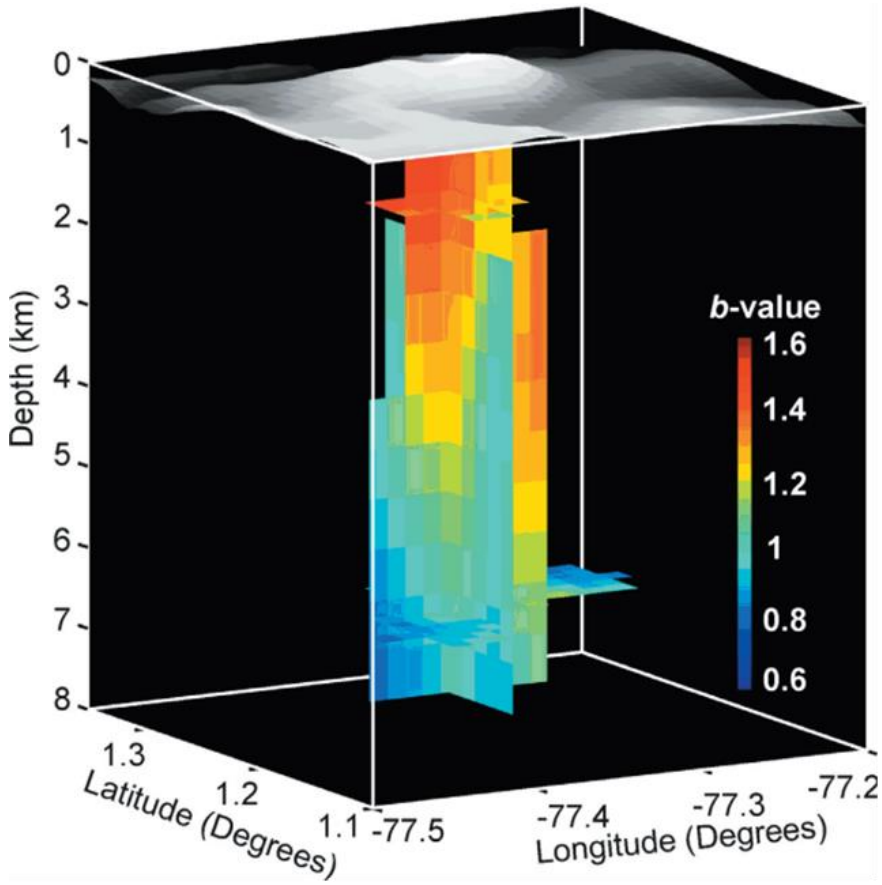

Figure 12 Three-dimensional view of the distribution of b value in Galeras Volcano. Taken from Sánchez et al., 2005.

3.2 Gravimetric Studies

Ortega (2014) employed 286 stations, including distant stations to minimize the effects of borders, distributed in an area of 1200 km^2 surrounding the volcano, to determine the anomalies or variations in gravity generated by the contrasts in density of bodies located irregularly in depth. The sources of these anomalies can be regional (deep), possibly due to the basement of the volcanic edifice or residual (local), located at intermediate or superficial levels. Separating these two components is possible thanks to several mathematical and analytical processes, which must go hand in hand with the geological understanding of the area. To estimate the evolution of the behavior of the Bouguer anomaly in depth, analytical upwards continuations for heights of 500 m, 1400m, 2800 m, 4200, and 5600 m were made. These maps show how the regional anomaly is changing shape at depth and losing the most superficial features, becoming circular with a concentric pattern. This represents a gravimetric low whose mass center would be at depths greater than 5 km, associated with a deep regional source. The iso-anomaly lines denote the possible volcanic conduits.

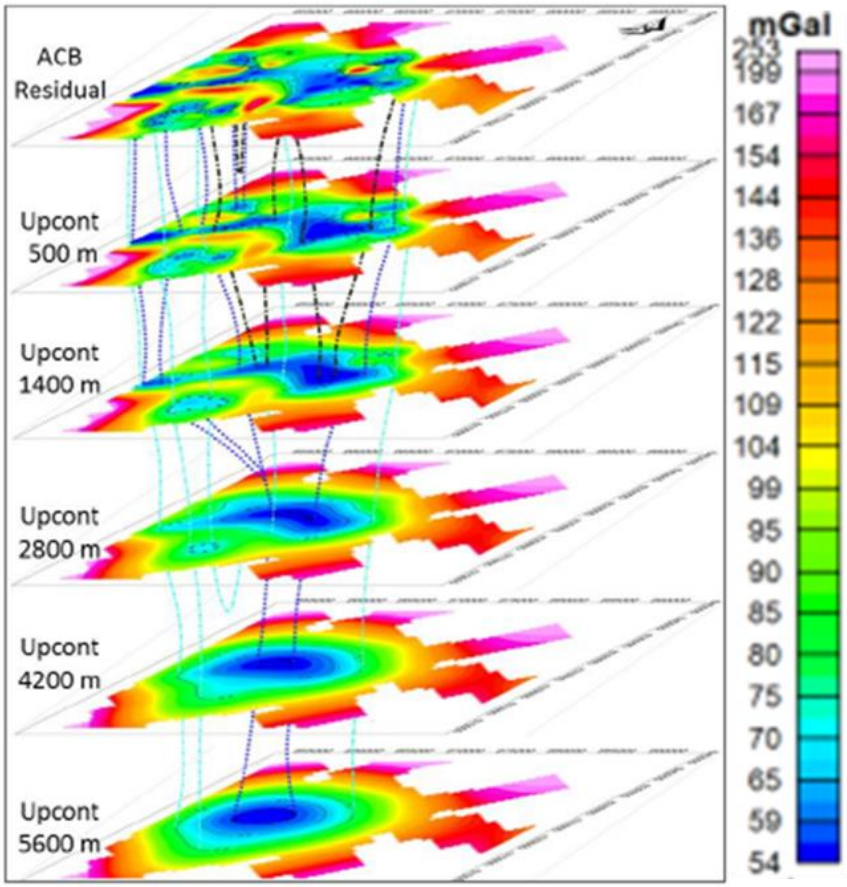

Figure 13 Bouguer Anomaly in Galeras Volcano area and its analytical upwards continuations, heights of 500 m, 1400m, 2800 m, 4200, and 5600 m, taken from Ortega, 2014.

From the residual anomaly map, two gravimetric low zones stand out (Figure 14): one in the crater region, which extends to the east, and one in the W zone, possibly associated with deposits of poorly consolidated material generated by debris avalanches and mudflows (Ortega, 2014). On the other hand, a gravimetric high is recognized located towards the NE of the crater, that adjusts with the presence of a zone of high velocity, previously associated with a more compact or rigid medium than its surroundings (Torres, 2012). Other high gravimetric SW and NW zones are associated with the presence of the oldest volcanic formations like Cariaco and Pamba (Ortega, 2014).

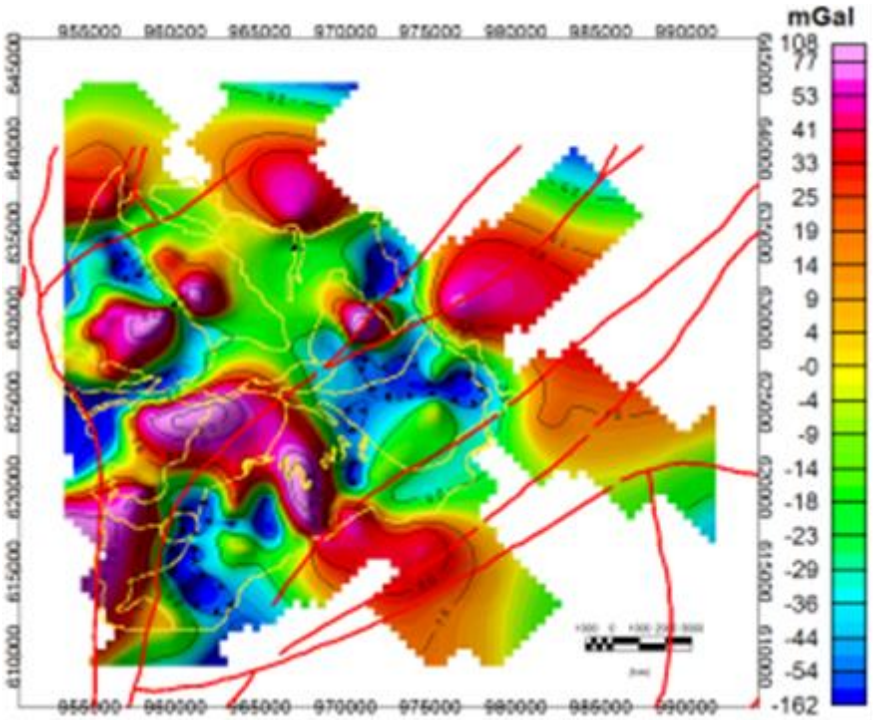

Figure 14 Residual Gravimetric Anomaly Map in Galeras Volcano area, taken from Ortega, 2014.

4 DISCUSSION

4.1 Scope and Limitations

A geothermal system can be understood as the coexistence of a heat source, permeable hot rock body and a geothermal fluid, all within a specific geological environment. The heat source or thermal anomaly is conventionally (in volcanic environments) associated with high temperature magma (≥600 ºC) located in the earth's crust, such as a cooling intrusion, a magmatic chamber or a caldera located at shallow depths (< 10 km). A body of hot rocks constitutes the reservoir where the energy in form of heat is stored, and the fluid acts as a transport mechanism of this caloric resource. Generally, the system is connected to the surface through structural features such as faults and fractures, this connection maintains a dynamic recharge and discharge of the fluid. Ideally this system should be covered by an impermeable barrier that prevents the loss of heat by circulation of the geothermal fluid to cold lithologies. This barrier is called a seal layer. Figure 15 is a schematic representation of an ideal geothermal system. Any study of recognition and pre-feasibility of geothermal potential must be aimed to corroborating the existence or not of each of the constituents of the geothermal system, providing a first approach to the quantitative and qualitative characterization of each of these elements, as well as their dynamics and interactions from depth to surface considering all available scientific information, although this document does not fully resolve all these questions it is intended as a basis for future achievement.

The multiple documents, reports, and scientific *papers* that have been consulted are mainly focused on volcanic monitoring and the understanding of pre-eruptive dynamics for risk management in Galeras Volcano area and the petrographic characterization and modeling of the magmatic system, among others. This analysis highlights the most relevant aspects with a geothermal approach, taking as a base the same information.

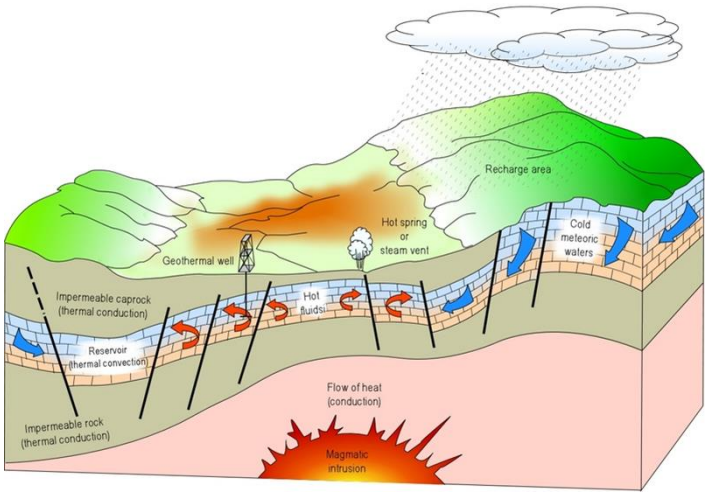

Figure 15 Scheme of an ideal geothermal system. Taken from Dickson and Fanelli 2004

4.2 Joint Analysis

Tectonically the region is characterized by the presence of active faults, highlighting the Romeral Fault System, predominantly inverse and with a high dip angle and a component of dextral movement in the Galeras Volcano area (Taboada et al., 1998). The eastward migration of eruptive centers and the recording of fissure events on the east flank of the edifice confirm a marked tectonic control over volcanic activity and it is expected that this same fault system controls the lateral extension of a hypothetical subsurface reservoir. Evidence from strongly altered rocks in the collapse scars suggests the circulation of hydrothermal fluids from the system as a process that contributes to the development of instability in the volcanic edifice. The mapping of hydrothermal manifestations and local structural features in Galeras Volcano is scarce and does not set (but does not rule out) the relationship that typically exists between these two features; a detailed structural study is necessary to recognize fracture families, density, frequency, geometry, identify microstructural units, their limits and dynamics.

The volcanostratigraphy of the Galeras Volcanic Complex defines large extensions of andesitic lavas and pyroclastic deposits, with thicknesses of up to 500 m representing the first phase of Cenozoic volcanism (Cepeda, 1986). According to regional stratigraphy, these rocks lie on the Esmitia Formation, described as intercalations of limestones, sandstones, conglomerate sandstones and polymict conglomerates (León et al., 1986, 1979). Therefore, the Esmitia Formation must be considered together with the large levels of andesitic lavas as the possible lithologies that by primary and secondary permeability, respectively, could become potential storage levels of geothermal fluid. In parallel, the hydrothermal alteration (to be verified), in the pyroclastic levels of the same volcanic successions, could contribute to the development of the seal layer in the system. The global composition of the volcanic provents is almost constant: andesites calc-alkaline, rich in silica and medium in potassium content; chemical and petrographic analyses indicate the presence of andesites (91 %), basaltic andesites (3.5%) and dacites (5.5 %) (Cortés & Calvache, 1997) suggesting the existence of a magmatic source with an average degree of differentiation and crust contribution. Petrographically the porphyritic texture predominates, being plagioclase, amphibole, orthopyroxene and clinopiroxene the most common minerals; titanomagnetite, ilmenite apatite and olivine as accessory minerals.

The fumarolic manifestations are limited to the vicinity of the active crater of Galeras Volcano (Figure 2) and do not behave homogeneously. Particularly, the Deformes fumarole presents the greatest variation in its discharge temperature (Figure 3), evidencing the mixture with gases from the hydrothermal system and possibly meteoric water. Conversely, the Besolima and Florencia fumaroles located along the trace of the RFS present higher and more uniform temperatures (even > 300 ºC) suggesting a

rapid ascent, free of mixing. The hot springs associated with the GV hydrothermal system present low discharge temperatures (maximum 31 ºC) even near the crater. Fischer et al. (1997) identified dilution of a common source for acid-sulfate waters; a great variation in the chemical composition over time in the source of Aguas Agrias pointing towards the immaturity of the waters. Further, the geothermometers consulted present a very wide range of temperatures, supporting the idea that the Galeras Volcano has an immature hydrothermal system. Other chemical indicators such as Li and B content (Appendix A) do not suggest the contribution of a geothermal fluid in surface discharges.

The 1-D velocity model used by the Galeras Volcano tomography proposes two zones at 4 km deep (with respect to the summit) with the lowest P and S wave velocities, which for a volcanic environment could correspond to intensely altered or fractured pyroclastic and lavas deposits. Velocities increase with depth. It is worth mentioning that the models generated by Carcolé et al (2006), Torres (2012) and Sánchez et al (2005) are valid until the first 10 kilometers of depth since almost none of the hypocenters used in their investigations exceed this depth. The Galeras Volcano seismic tomography highlights two areas of low P and S velocities: to the NW and SE of the active crater, the absence of volcanotectonic events (generally associated with stress or shear fractures, induced by pressure) indicate these two as regions of higher temperature (no brittle behavior) with partially melted material or intense hydrothermal alteration; the depth of these anomalies (< 3 km) suggests the second scenario. The concentration of several hypocenters of VT earthquakes that align vertically under the main crater up to a depth of about 4 km, linked to higher values of P wave velocity and high values of parameter b with respect to its sides, suggests a vertical structure of brittle behavior, possibly associated with remaining intrusive bodies, transitory reservoirs of magma or material ascent vents. NE of the main crater, an agglomeration of VT hypocenters between 4 and 6 km deep below the Buesaco and Silvia-Pijao Faults alignment is identified, as well as an anomaly of high P wave velocity between 0 and -2 km with the VT hypocenters of greater magnitudes, all this could be associated with the existence of solidified intrusive bodies that have extended along the Silvia - Pijao and Buesaco fault lineaments.

The seismic tomographies of greater penetration agree in the presence of two anomalous zones associated with two magmatic chambers; a shallow one (4 km) connected by a system of fractures to a deep chamber (> 9 km) that feeds it permanently (Moncayo, 2004). The geophysical model for the internal structure of Galeras Volcano that best agrees with all the studies is proposed by Torres (2012). It involves the results of seismic tomography and the distribution of volcanotectonic events. Figure 16 presents two schematic cross sections that illustrate this model along the GV in parallel and perpendicular direction of the Buesaco fault, respectively.

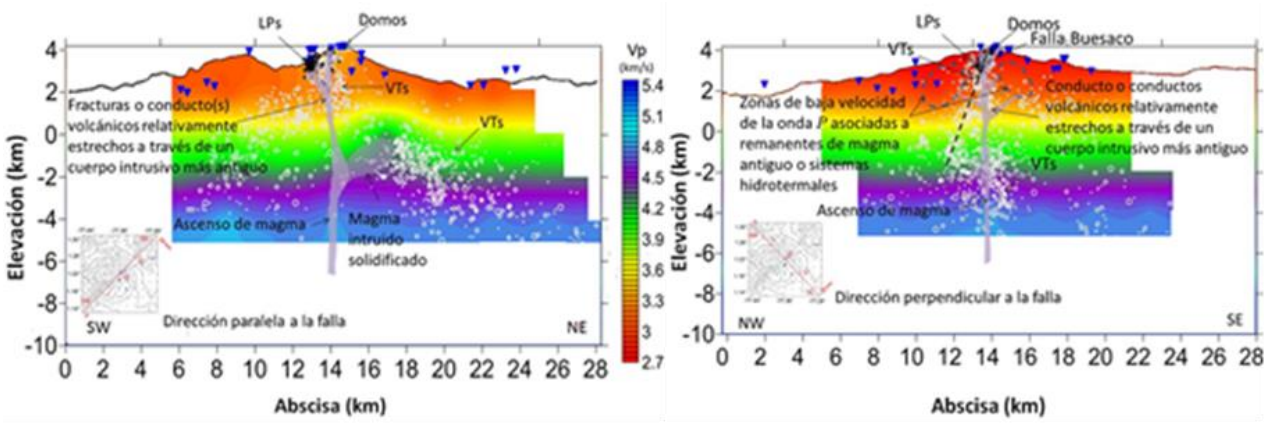

Figure 16 Conceptual geophysical model of the internal structure of Galeras Volcano. Left cross section SW - NE, right cross section NW- SE Taken from Torres (2012).

Based on the joint analysis and in agreement with all the studies consulted, a preliminary conceptual geothermal model for Galeras Volcano is proposed (Figure 17), defining a volcanic vent that is elongated vertically, extending about 5 kilometers deep, where there is a transitory magmatic chamber, with crust contribution and moderate differentiation. This shallow magma chamber is fed through a system of fractures and volcanic vents by a main magmatic chamber of primary composition with an estimated depth greater than 9 km. The lineament of the Buesaco Fault together with the presumable families of faults and fractures define the structural configuration that conditions the circulation pattern of fluids in the subsurface. This pattern must justify the location and discharge temperature of the main hydrothermal manifestations in the area. The location of NW and SE anomalies associated to areas with higher temperatures and/or a high hydrothermal fluid content, is also presented, recommending them as the most promising regions for future geothermal pre-feasibility studies.

5 CONCLUSIONS AND RECOMMENDATIONS

5.1 Conclusions

The large layers of andesitic lavas genetically associated with the evolution of the Galeras Volcanic Complex and the immediately underlying Esmitia Formation are lithologies that could constitute a geothermal reservoir by secondary and primary permeability, respectively. The levels of pyroclastic deposits in the area are frequent and powerful; if there is a sufficiently developed hydrothermal alteration, these horizons could act as a seal layer for the geothermal reservoir.

The migration of eruptive centers eastward and the recording of fissure events on the east flank of the edifice confirm a marked tectonic control over volcanic activity and it is expected that this same fault system controls the lateral extension of a hypothetical subsurface reservoir. The register of explosive events, of phreatic genesis indicates the existence of groundwater, possibly linked to an aquifer, or in the best case a geothermal reservoir, but also marks the capacity of the GV to generate large and dangerous events.

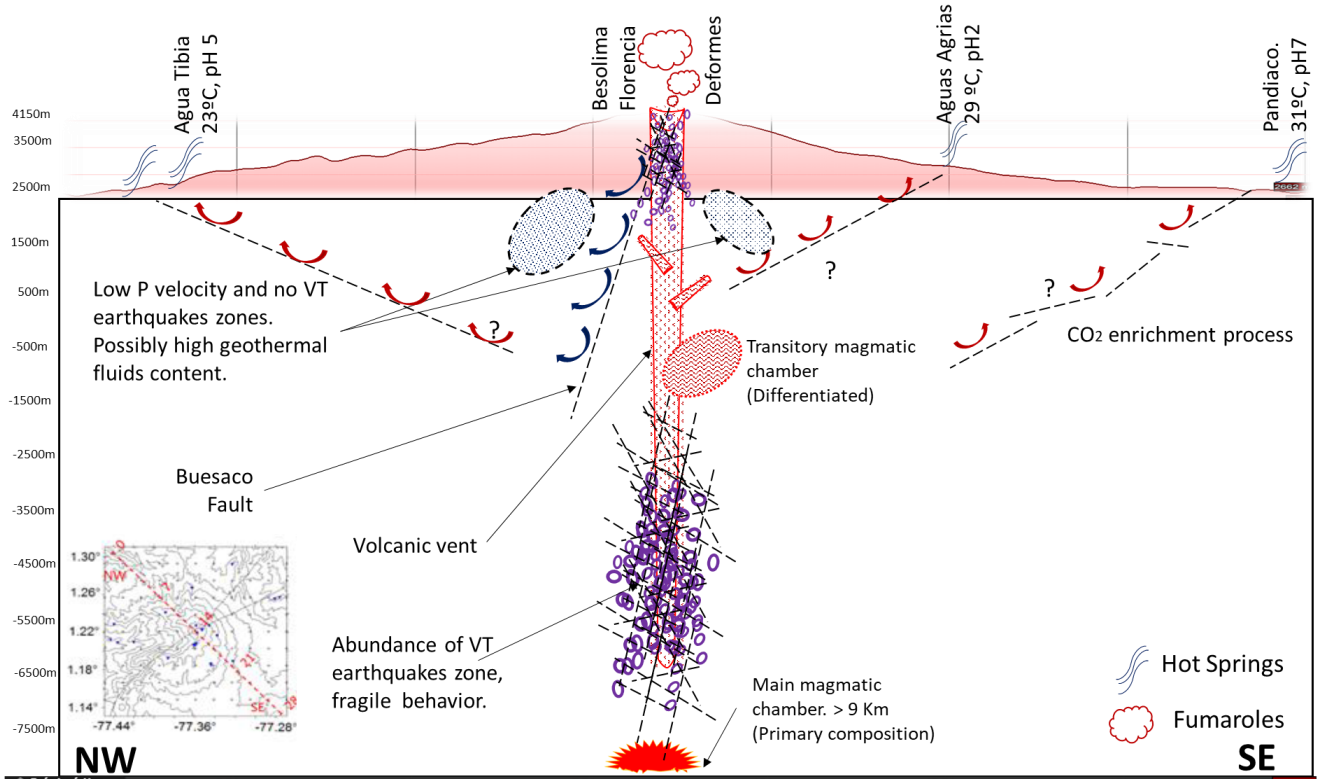

Figure 17 Preliminary conceptual geothermal model for Galeras Volcano, highlighting in black ovals the two areas of greatest interest.

In general, geophysical studies are congruent with each other, defining an elongated form from the crater to almost 5 km deep, with high P-wave velocity, concentration of VT events and high b-parameter values. This feature is associated with a remnant magma reservoir or (more likely) an ascent vent. The NE anomaly zone between 4 and 6 km deep, with an agglomeration of VT registers and high P wave velocities, indicates the existence of solidified intrusive bodies that extended throughout the Romeral Fault System.

The areas of low velocity P and S waves, with the absence of VT earthquakes to the NW and SE of the volcanic edifice should be highlighted as those with greater geothermal interest. They are possibly associated with intense hydrothermal alteration (an eventual seal layer) or with the circulation of hot fluids less than 2.5 km below the surface.

5.2 Recommendations

There are multiple geochemical indicators that indicate the immaturity of the hydrothermal system in Galeras Volcano, however, the existence of an active heat source is evident. A dedicated study is necessary, with a robust geochemical sampling to better understand the dynamics of magmatic and hydrothermal fluids.

A detailed structural study of the Galeras Volcano area is recommended to recognize fracture families, density, frequency and fault geometry, identify microstructural units, their limits and dynamics.

The GV proximity to a large populated center such as Pasto should motivate investment in integral studies that enrich the understanding of eruptive dynamics to improve volcanic risk management, while supporting the process of geothermal prospecting. Besides, in order to stablish a reliable and accurate “Colombia’s Geothermal Inventory”, it is necessary to make a first approach towards the preliminary characterization of geothermal potential in other less-studied systems.

REFERENCES

Anderson Jr. A. 1991. Subvolcanic degassing of magma. Magmatic Contributions to hydrothermal systems and the behavior of volatiles in magma. Geol. Surv. Jpn. Rep., 279: 213.

Bhattacharyya. (1966). Continuous spectrum of the total-magnetic-field anomaly due to a rectangular prismatic body. Geophysics.

Calvache, M. & Cortés, G. (1997). Stratigraphy and Chronology of the Galeras Volcanic Complex, Colombia. Journal of Volcanology and Geothermal Research

Calvache, M. (1995). The geological evolution of Galeras Volcanic Complex. Arizona State University.

Calvache, M. L. (1990). Geology and volcanology of the Recent Evolution of Galeras Volcano, Colombia. Louisiana State University.

Calvache, M., & Williams, S. (1991). The last 4500 years of Galeras Volcano, Nariño, Colombia. Symposium on Andean magmatism and its tectonic frame.

Carcolé, E. (2006). Three-dimensional spatial distribution of scatterers in Galeras volcano, Colombia.

Cepeda, H. & Ordóñez, M (1996) Morphological changes of the active cone of Galeras Volcano, Colombia, during the last century. Journal of Volcanology and Geothermal Research

Cepeda, H. (1986). Petrological investigations in the scope of the plates 429-Pasto and 410.Ña Union, with special emphasis in the Volcanic Complex Galeras. . Bogotá: INGEOMINAS.

Chouet, B., 1981. Ground motion in the near field of a fluid driven crack and its interpretation in the study of shallow volcanic tremor. Journal of Geophysical Research, 86: 5985-6016.

Chouet, B., 1988. Resonance of a fluid-driven crack: radiation properties and implications for the source of long-period events and harmonic tremor. J. Geophys. Res., 93: 4375-4400.

Chouet, B. (1992). A seismic model for the source of long-period events and harmonic tremor. Berlín: Springer-Verlag.

Chouet, B. (1996). Long-period volcano seismicity: its source and use in eruption forecasting. Nature.

Cortés, J., & Calvache, M. (1997). A synthesis of the recent activity of Galeras Volcano, Colombia: Seven years of continuous surveillance, 1989-1995. Journal of Volcanology and Geothermal Resources.

Espinosa, A. (2001). Historical Eruptions of Colombian Volcanoes (1500-1995). Bogotá: Colombian Academy of Exact, Physical and Natural Sciences.

Fischer, T.P., Arehart, G.B., Sturchio, N.C. & Williams, S.N.: (1996) The relationship between fumarole gas composition and eruptive activity at Galeras Volcano, Colombia. Geology 24, 531–534Frolich, C., & Davis, S. (1993). Teleseismic b-values: Or much ado about 1.0. Journal of Geophysical Research.

Fischer, T.P., Sturchio, N.C., Stix, J., Arehart, G.B., Counce, D., & Williams, S.N.: (1997) The chemical and isotopic composition of fumarolic gases and spring discharges from Galeras Volcano, Colombia. Journal of Volcanology and Geothermal Research, 77, 229-253.

Giggenbach, W.F. and Goguel, R.L., 1988. Methods for the collection and analysis of geothermal and volcanic water and gas samples. Dep. Sci. Ind. Res. Chem. Div. Rep. CD 2387, 53 PP.

Giggenbach, W. (1992). The composition of gases in geothermal and volcanic systems as a function of tectonic setting.

ISAGEN. (2014). Geothermal Energy Entrepreneurship in Colombia.

Latter, J. (1979). Volcanological observations at Tongariro National Park, 2. Types and classification of volcanic earthquakes. Department of Scientific and Industrial Research, Geophysics Division, Wellington, New Zealand.

López, D., & Williams, S. (1993). Catastrophic volcanic collapse: relation to hydrothermal processes.

Meissner, R. e. (1977). Dynamics of the active plate limit in the SW of Colombia.

Mogi, K. (1962). Magnitude-frequency relation for elastic shocks accompanying fractures of various materials and some related problems in earthquakes. Tokyo: Bulletin of the Earthquake Research Institute.

Murcia, A., & Cepeda, H. (1991). Geological Map of Colombia. Plates 429 - Pasto, Department of Nariño. Scale 1:100,000. Bogotá: INGEOMINAS.

OLADE. (1982) Study on the recognition of geothermal resources in the Republic of Colombia. Colombian Institute of Electric Energy.

Ortega, A. (2014). Model of regional and local gravimetric anomaly sources of the Galeras volcano, associated with its June 2008 - April 2009 activity. Bogotá: National University of Colombia.

Sánchez, J. (2004). Spatial variations in the frequency-magnitude distribution of earthquakes at Mount Pinatubo Volcano. Bulletin of the Seismological Society of America.

Sánchez, J. (2005). Spatial Mapping of the b-Value at Galeras Volcano, Colombia, using earthquakes recorded from 1995 to 2002.

Scholz, C. (1968). The frequency-magnitude relation of microfracturing in rock and its relation to earthquakes. Bulletin of the Seismological Society of America.

Spector, A., & Grant, F. (1970). Statistical models for interpreting aeromagnetic data. Geophysics.

Stix, J., & Calvache, M. (1997). Galeras Volcanic Complex, Colombia, Introduction to an Interdisciplinary Study of a Decade Volcano.

Symonds, R., & Reed, M. (1993). Calculation of multicomponent chemical equilibria in gas-solid-liquid systems: Calculation methods, thermochemical data, and applications to studies of high-temperature volcanic gases with examples from Mt. St Helens.

Taran, Y., & Pokrovsky, B. (1989). Deuterium and oxygen-18 in fumarolic steam and amphiboles from some Kamchatka volcanoes.

Torres, R. (2012). Galeras Volcano 3-D Model using Seismic Tomography. Bogotá: National University of Colombia.

Vargas, C. (2006). Coda Q tomography at Galeras Volcano, Colombia. National University of Colombia.

Warren, N., & Latham, G. (1970). An experimental study of thermally induced microfracturing and its relation to volcanic seismicity. Journal of Geophysical Research.

Wiemer, S., McNutt, S.R, & Wyss, M. (1998). Temporal and three-dimensional spatial analysis of frequency-magnitude distribution near Long-Valley caldera, California. Geophysical Journal International. 134, 409-421

Wyss, M. (1973). Towards a physical understanding of the earthquake-frequency distribution. Geophysical Journal of the Royal Astronomical Society.

Appendix A: Chemical composition (mmol/mol Dry steam) and carbon and nitrogen isotopes in the fumaroles of Galeras Volcano. Taken and modified from Fischer et al., 1997

Ubicación	Fecha (yymmdd)	Muestra	T (ºC)	CO2	S(tot)	HCl	HF	He	H2	CO	Ar	O2	N2	CH4	13C	15N	H20 (wt.%)
Calvache	881215	B4-C	88	664	430	0,1		0,004	0,30	< 0.02	0,00	0,00	5,0	0,002			92,20
Gal Crater	891212	#2	225	427	524	41,6		0,003	3,10	< 0.02	0,01	0,00	4,7	0,003			93,40
Galeras	891215	#3	225	486	443	56,8		0,003	1,60	<0.02	0,11	1,37	11,1	0,003	-5,8		94,50
Deformes	900106	AO	187	390	404	125,9		0,016	0,50	< 0.02	0,85	4,39	74,0	0,008			94,30
Defonnes	900209	#4	227	371	348	33,1		0,030	12,70	< 0.02	2,	15,94	216,9	0,125			93,80
Deformes	900808	B2	243	549	385	56,6		0,003	3,10	< 0.02	0,02	0,03	6,9	0,013	-6,2		91,70
Galeras	900808	B3		648	329	7,1		0,005	4,90	< 0.02	0,03	0,02	10,6	0,082			90,50
Galeras	900809	C4		595	371	19,5		0,003	4,80	< 0.02	0,04	0,04	9,5	0,051	-6,2		92,10
Galeras	910901	B3	249	627	300	44,7		0,001	13,50	< 0.02	0,04	0,06	14,7	0,092			94,10
Deformes	920625	Dell	218	729	247	2,4		0,002	7,70	< 0.02	0,02	0,00	13,7	0,004	-7,4	2,7	95,70
Deformes	920708	Deft	213	832	108	1,3		0,005	4,30	< 0.02	0,15	0,10	54,2	0,010	-7,4	2,7	98,20
Deformes	920804	Def (#17)	222	875	105	1,3		0,004	2,70	< 0.02	0,05	0,02	16,3	0,004	-4,6	5,3	93,50
Besolima	920626	Besl	397	633	161	54,5		0,004	4,60	< 0.02	2,	27,53	167,3	0,020	-5,9	0,1	96,10
Besolima	920708	Best	230	791	162	3,0		0,004	32,70	< 0.02	0,02	0,02	11,6	0,006	-5,0	4,7	98,70
Deformes	921126	unknown	230	764	175	52,9			0,90	0,02		0,00	6,3				93,00
Florencia	921126	unknown	642	702	166	83,6	7,30		33,50	1,60			4,8	0,002			91,50
Defonnes	930114	unknown	200	726	239	27,4	0,96	0,015	0,40	< 0.02	0,04	0,00	5,7	0,000			97,70
Deformes	930130	GS 2-2	194	692	277	25,5	0,86	0,036	0,50	< 0.02	0,04	0,00	3,7	0,000			97,80
Deformes	930130	0V93-32B	194	714	238	37,6	1,64	0,015	0,80	< 0.02	0,01	0,00	6,0	0,007			97,90
Besolima	930202	GS5-2	358	768	128	58,3	0,43	0,004	32,30	0,23	0,27	0,02	13,3	0,293	-6,0	3,6	96,40
Besolima	930202	0V93-35A	358	751	161	23,7	3,46	< 0.001	30,90	1,	0,19	0,00	21,8	0,000			99,70
Besolima	930202	0V93-35B	358	753	175	37,0	3,66	<0.001	22,80	0,31	0,01	0,00	4,6	0,000			99,70
Chavas	930212	GS7-1	164	623	347	11,1	0,69	< 0.001	0,40	< 0.02	0,20	0,11	16,4	0,000			91,60
Deformes	930212	058-1	197	591	359	35,5	0,27	0,019	0,50	< 0.02	0,03	0,34	12,7	0,000	-10,4	2,7	95,10
Respirador	930125	051-1	-	864	<1	< 0.1	< 0.04	5,027	3,80	<0.02	1,	25,32	102,5	0,000			94,10
Roca	930224	GS I2-1	-	998	<1	< 0.1	< 0.04	0,038	3,80	< 0.02	0,02	0,34	1,3	0,018			98,90
Pandiaco	930403	GS18-1	-	988	<1	< 0.1	< 0.04	< 0.001	3,80	< 0.02	0.1 I	2,30	9,3	0,012	-18,1	5,6	76,00
Deformes	940721	0S94- 1	140	437	404	129,4		< 0.001	0,20	< 0.02	0,10	0,00	26,9	0,000			97,00
Deformes	940808	0S94-2	140	423	424	130,1		< 0.001	0,90	< 0.02	0,09	0,00	25,9	0,000			94,70
Defonnes	950707	Defja1795	145	857	112	17,6	0,18	0,002	0,20	0,002	0,01	0,03	12,9	0,010	-8,5		91,40
Chavas	950715	NJ11595	416	405	147	23,9	0,18	< 0.01	192,90	0,03	5,40	< 2.04	224,3	0,429	-8,7	57,2	
Deformes	951212	Def1295	145	875	106	6,6	0,15	0,001	2,00	0,02	0,03	0,05	10,9	0,028	-7,9	93,4	

Appendix B: Table 2 Isotopic composition of gas samples from Galeras Volcano. (Fischer et al., 1997)

Fumarola	Fecha (yymmdd)	T (°C)	18O (‰)	2H (‰)
Deformes	920625	218	-0,4	-56
Deformes	920702	204	1,8	-48
Deformes	920708	213	-0,8	-54
Deformes	920814	222	0,3	-54
Deformes	930130	194	-3,3	-57
Deformes	930212	167	-4,1	-58
Deformes	940721	140	-3,3	-66
Deformes	940808	140	-3,4	-67
Deformes	950707	145	-5,3	-72
Deformes	950708	145	-6,0	-77
Deformes	950724	145	-4,4	-68
Deformes	951011	149	-5,9	-75
Deformes	951122		-7,0	-82
Deformes	951212	145	-5,0	-71
Besolima	920626	397	2,2	-39
Besolima	920703	145	1,8	-40
Besolima	920708	230	4,9	30
Besolima	920727	431	4,3	-34
Besolima	930202	360	1,9	-39
Besolima	930202	360	3,6	-39
Chavas	950715	410	1,9	-49
Chavas	950715	410	2,1	-51
Chavas	951011	416	1,5	-56
Chavas	951122	416	1,3	-57
Chavas	951212	416	1,4	-53